Plasmonic enhancement of one-photon- and two-photon-excited single-molecule fluorescence by single gold nanorods

Zhang, W.

1

Introduction

In this chapter, we introduce the fundamental physics involved in the thesis and the motivations of the current studies. It includes a general introduction on linear and nonlinear fluorescence, and fluorescence enhancement using plasmonics nanostructures with the focus on gold nanorods. Finally, we give an outline of the different chapters in this thesis.

1

1.1. Light absorption and emission

The emission of ultraviolet, visible or infrared photons from an electronically excited species is called luminescence. The excitation energy can be from chemical reactions, electric energy, light, *etc*. If the excitation is achieved by absorption of photons, the subsequent emission is then called photoluminescence. Natural materials that show photoluminescence include minerals and tissues in plants and animals. Nowadays, artificial photoluminescence materials with superior optical performances are synthesized and widely used in photoluminescence-based applications. These materials present high emitting brightness, a broad variety of colors, and good bio-compatibility. Prominent examples include synthetic organic dyes, semiconductor nanocrystals (quantum dots), and fluorescent proteins. They have become dispensable tools for biological and analytical chemical studies. In the following, we will describe in detail the processes involved in the generation of photoluminescence, with a focus on that from organic dyes.

1.1.1. Jablonski diagram

Light absorption and emission by a molecule in solution involve the electronic transition to an excited state S_1 and the subsequent relaxation to the ground state S_0. The relevant processes are schematically illustrated by a Jablonski diagram shown in Fig. 1.1. The electronic transition can be promoted in a few different ways, which will be elaborated later. The excited state can be deactivated to the ground state by emitting a photon in a time scale of sub-nanosecond to $\sim$ 10 ns for typical dye molecules. This photon emission is called fluorescence. However, not every electronic transition results in a photon emission. Other relaxation pathways compete with the fluorescence emission process, making the quantum yield (QY) of light emission less than unity. For example, the excited state energy can be dissipated as heat through nonradiative decay. Alternatively, the excited molecule can interact with another molecule to transfer energy (thereby quenching the fluorescence) or go to the lowest excited triplet state (T_1) via intersystem crossing. The sum of the decay rates of all the deactivation pathways defines the excited state lifetime.

The triplet state T_1 , which has typically microsecond lifetime, is usually a dark state at room temperature, namely, the decay from T_1 to S_0 is nonradiative. Therefore, the molecule may enter a nonfluorescent state periodically, a phenomenon known as fluorescence blinking. (At low temperature, the triplet state can also be deactivated radiatively, a process called phosphorescence. Fluorescence and phosphorescence are particular cases of luminescence.) After an internal relaxation in the ground state, the molecule is ready for another absorption-emission cycle. Most fluorophores can repeat the excitation and emission cycle many times. However, the excited states (especially the triplet excited state) are more reactive with the surrounding which can result in photobleaching: the molecule is permanently transformed and becomes unable to fluoresce. The characteristic on-off blinking and one-step blinking are important criteria to identify single molecules in single-molecule studies, which will be discussed later.

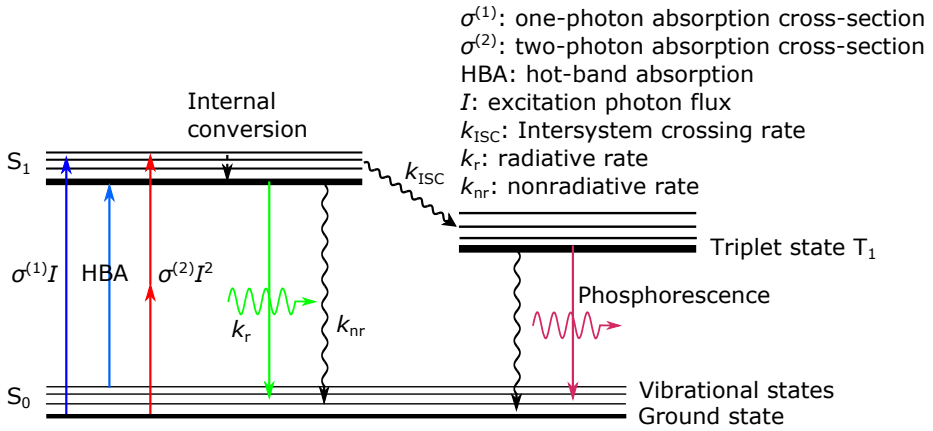

Figure 1.1: **Jablonski diagram** depicting the electronic states involved in the process of light absorption and emission.

1.1.2. One-photon-excited fluorescence

In the simplest and most conventional case, optical excitation is achieved by absorbing one single photon. Depending on the energy of the excitation photon, the molecule may be excited to higher vibration levels of the S_1 state or even to the S_2 state. The excitation rate is a linear function of the excitation photon flux I (cm^{-2} s^{-1}) in the weak excitation range below saturation, *i.e.*, $k_{exc}^{(1)} = \sigma^{(1)} I$, where $\sigma^{(1)}$ is the one-photon absorption cross-section ($\sim 10^{-16}$ cm^2 for most dyes). After excitation, the molecule relaxes to the lowest energy level of the relaxed S_1 state via a rapid ($< 10^{-12}$ s) nonradiative internal conversion. Afterwards, fluorescence is emitted from the lowest level of S_1 state irrespective of the excitation wavelength. Therefore, the emission spectra of fluorophores are usually independent of the excitation wavelength. Also, the emission is at longer wavelengths than the excitation photon because of the energy dissipation in vibrational relaxation in both the excited and ground states.

1.1.3. Two-photon-excited fluorescence

Fluorophores can also be excited by the simultaneous absorption of two photons, each with lower energy than that required for one-photon excitation, as depicted in Fig. 1.1. No intermediate states are involved. The selection rules for two-photon absorption (TPA) are different from those of for one-photon absorption, therefore the molecules may be excited to different excited states. However, the molecules emit from the lowest level of the S_1 state, independent of one- or two-photon absorption. All the molecules examined to date display the same emission spectra and lifetimes as if they were excited by one-photon absorption [1].

The first theoretical analysis of TPA dates back to 1930s when Maria Goeppert-Mayer predicted TPA in her doctoral dissertation. But it was only 30 years later that TPA was experimentally demonstrated, largely thanks to the invention of lasers. Due to the requirement

of the nearly simultaneous absorption ($\sim 10^{-16}$ s) of two photons [2], the probability of occurrence of TPA is low, *i.e.*, the cross-section of TPA ($\sigma^{(2)}$) is low. Nowadays, femtosecond lasers are commonly used in conjunction with tight focusing geometries for TPA. The high peak energy of femtosecond lasers ensures a large number of excitation photons to achieve fluorescence emission from two-photon absorption.

Since the establishment of the first two-photon microscope in 1990 [3], the application of two-photon fluorescence in biological fields has been growing rapidly because of its advantages over one-photon fluorescence [2–6]. The emission spectrum of TPA is identical to one-photon fluorescence, but the excitation is at a longer wavelength than the emission, usually in the near-infrared region. Therefore, two-photon excitation is particularly suited for *in vivo* imaging due to the low absorption, autofluorescence and scattering of tissues in this wavelength range allowing for deep-tissue imaging (down to a few hundred micrometers). For TPA, the excitation rate is proportional to the squared incident light intensity, *i.e.*, $k_{\mathrm{exc}}^{(2)} = \sigma^{(2)} I^2$, where $\sigma^{(2)}$ is the two-photon absorption cross-section in terms of GM (Coppert-Mayer) units (1 GM = $10^{-50}\ \mathrm{cm^4 s\ photon^{-1}}$). (The $\sigma^{(2)}$ of common dyes is in the range of 1 - 300 GM [7–9]. There have been efforts to synthesize fluorescent molecules with higher two-photon absorption cross-sections. There is a growing literature on fluorophores with $\sigma^{(2)}$ values higher than 1,000 GM [10–14]. Semiconductor quantum dots usually have much higher $\sigma^{(2)}$ values (> 10^4 GM) [15].) As a consequence of the nonlinear response, excitation is confined to a small volume near the focal point. This leads to inherent sectioning without the need of using additional optical elements (*e.g.* a pinhole) to reject the out-of-focus emission, which leads to higher light collection efficiency. Additionally, photobleaching and photodamage are then localized to the focal plane, which may allow imaging of living specimens over longer time periods than one-photon excitation, where photobleaching and photodamage occur across the entire thickness.

1.1.4. Hot-band absorption induced anti-Stokes luminescence

In this thesis, we also studied a special kind of light excitation termed hot-band absorption, which was first observed in 1928 [16]. A molecule can be excited from a thermally populated high vibration energy level ("hot band") by photons with longer wavelength (lower energy) than the emission wavelength to reach the excited state. The molecule then decays from the excited state back to the ground state in a same manner as in normal fluorescence. Consequently, the emission profile is the same as common fluorescence. Like two-photon fluorescence, hot-band absorption induced luminescence has anti-Stokes shift from the excitation wavelength, but hot-band absorption is a linear process. No ultrafast laser is required. From the energy conservation point of view, the additional energy is provided by the thermal energy originated from the original Boltzmann distribution of the dye molecules.

1.2. Single-molecule fluorescence spectroscopy

As discussed above, fluorescence is emitted at a different wavelength than the excitation photons. Moreover, fluorescence emission is generally a much slower process than Rayleigh or Raman scattering, which occurs on a femtosecond scale. Therefore, fluorescence signals can be well separated from background in both the time and frequency domains. These

properties grant fluorescence microscopy high contrast and sensitivity. Fluorescence is capable of selectively detecting exceedingly low concentrations of molecules, down to the single-molecule level.

The first single-molecule fluorescence detection was demonstrated by Orrit and Bernard in 1990 [17] in cryogenic solids. It marked a major breakthrough in the field of optics. It greatly extended the scope of fluorescence microscopy, providing unprecedented insights into complex systems where static and dynamic heterogeneity is present [18–20]. Single fluorescent molecules are nano-scale probes for studying soft matter systems and biological mechanisms, revealing molecular dynamics with an unprecedented level of detail that may otherwise be buried in ensemble averaging in conventianal bulk measurements. Since its invention, single-molecule spectroscopy has led to several break-throughs in fundamental studies of physical and chemical phenomena and biological processes controlled by macromolecules [21], such as RNA folding [22] and protein folding [18, 23].

1.3. Plasmonic nanoantennas and fluorescence enhancement

Current single-molecule spectroscopy studies mostly rely on the high contrast against background provided by fluorescence. It is therefore highly desired to have fluorophores with emission intensities as high as possible. The emission of an overwhelming majority of absorbers, however, can be extremely weak if non-radiative relaxation is much faster than spontaneous emission of the excited state, or if the transition is nearly forbidden, as happens in lanthanide ions. Compared with one-photon-excited fluorescence, two-photon and hot-band absorption materials are typically weaker emitters due to the lower absorption probabilities. The aim of the current study is to increase the emission of weak emitters by exploiting the localized surface plasmons of metallic nanoparticles. Weak emitters will then be bright enough to be detected and studied individually. We can thus generalize single-molecule fluorescence spectroscopy to weakly emitting species which are currently undetectable by conventional single-molecule techniques.

1.3.1. Localized surface plasmons

When the size of the metal is of the order of the wavelength of light, localized surface plasmons (LSPs) occur. LSPs are collective oscillations of conduction electrons in metallic nanoparticles. The system is analogous to a damped harmonic oscillator with a resonance eigenfrequency. If the excitation frequency is in resonance with the eigenfrequency of the system, the oscillation of the conduction electrons reaches a resonance known as localized surface plasmon resonance (LSPR). The LSPR can be directly excited by visible light and leads to strong absorption and scattering of the metal nanoparticle. The LSPR of metal nanoparticles (primarily gold and silver) of various morphologies has attracted much scientific attention [24–29] because it gives rise to remarkable optical properties and applications in many areas, including imaging [30], (bio-)sensing [31], and photothermal therapy [32–34].

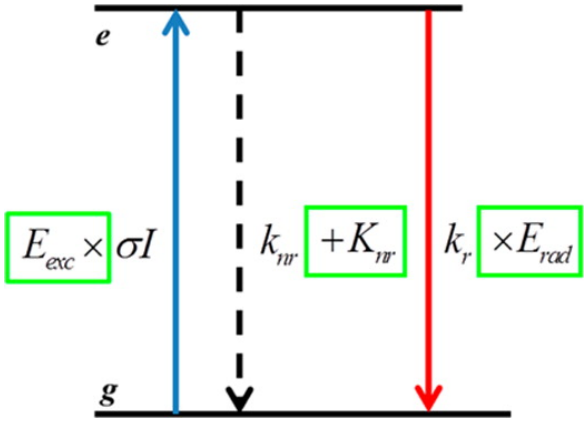

Figure 1.2: Simplified Jablonski diagram describing the transition rates of a molecule without and with (changes highlighted in green boxes) a nanoantenna. Reprinted from Ref. [39]

1.3.2. Fluorescence enhancement

It is well known that the emission rate of a quantum emitter (that emits only one photon at a time, *e.g.* a molecule or a quantum dot) is highly dependent on the local environment. Particularly, plasmonic nanoparticles (*e.g.* nanospheres, nanoshells and nanorods) have been used to work as nanoantennas to enhance the emission of adjacent emitters. See a good review on this topic [35]. As depicted in Fig. 1.2, considering a two-level model, such an enhancement involves a combined effect of three different near-field interactions between the emitter and the nanostructure [36, 37]. (i) Firstly, the excitation rate k_{exc} is increased because of the highly concentrated electromagnetic intensity at the vicinity of the nanoparticle. This part of enhancement is known as excitation enhancement E_{exc}. For one-photon excitation, the excitation rate enhancement is proportional to the enhancement of the local field intensity, while for two-photon excitation, the relation is quadratic. (ii) Secondly, plasmonic nanostructures enhance the spontaneous radiative rate (k_{r}) of neighboring emitters via the Purcell effect, leading to an increased spontaneous emission [38]. This contribution is called radiative enhancement (E_{rad}). (iii) Finally, the fluorescence may be quenched by energy transfer to dark modes of the nanoparticle and eventually converted to Ohmic heat in the metal. In other words, the nanoparticle opens up additional non-radiative decay pathways (K_{nr}) for the emitter.

The overall enhancement is a result of the complicated interplay between the three factors. Under weak excitation well below saturation, the overall enhancement is expressed as [39]

$$E_{\mathrm{all}} = E_{\mathrm{exc}} E_{\mathrm{rad}} \frac{k_{\mathrm{r}} + k_{\mathrm{nr}}}{k_{\mathrm{nr}} + K_{\mathrm{nr}} + E_{\mathrm{rad}} k_{\mathrm{r}}}.$$

E_{all} strongly depends upon the shape of nanoantennas, the emitter's position and orientation with respect to the antenna, and the overlap of its emission spectrum with the resonance of the antenna. Therefore, widely varying fluorescence enhancement dynamics have been reported for different emitter-nanoantenna systems [40–44].

1.3.3. Gold nanorods

Gold nanorods as plasmonic nanoantennas

Among many types of metallic nanoparticles, wet-chemically synthesized gold nanorods are the most extensively explored. They can be fabricated in a cheap way without the need of lithography or deposition equipments. A typical image of gold nanorods measured with scanning electron microscopy is presented in Fig. 1.3(a). Gold nanorods have relatively simple and well-defined morphology, which makes them easy to model and understand. Nanorods have two primary plasmonic modes: the transverse mode, where the plasmon oscillation occurs perpendicular to the major axis of the nanoparticle, and the longitudinal mode, where the plasmon oscillation is parallel to the major axis of the nanoparticle. Which of the modes is excited is determined by the alignment of the nanorod with the polarization of the incident light and the wavelength. The longitudinal LSPR is at a longer wavelength and more intense than the transverse LSPR and thus more often used [25].

Nanorods' narrow and strong longitudinal LSPR benefiting from the single-crystalline structure contribute to high fluorescence enhancement. Figure 1.3(c) shows the electric field intensity map around a nanorod whose longitudinal LSPR is excited. Strong electric field is concentrated at the tips of the nanorod. Moreover, the longitudinal LSPR is sensitive to the nanorod shape. Figure 1.3(b) shows the aspect-ratio (AR) dependence of the longitudinal LSPR. As the AR increases, the longitudinal LSPR becomes more intense and shifts from visible to near-infrared. This provides valuable parametric flexibility to study the plasmon-fluorophore system, *e.g.*, one can select the suited nanorods according the fluorophore for the best enhancement. Compared to nanogap antennas, such as bow-ties, dimers or particles on mirror, nanorods present a more open near field, which can accommodate molecules of various sizes. Important for biotechnological applications, gold nanorods are nontoxic and biocompatible [45]. Moreover, the gold surface has high reactivity towards thiol-modified molecules, allowing convenient chemical functionalization. For these advantages, we use gold nanorods to enhance fluorescence throughout the thesis. Systematic studies and precise understanding of the interaction of quantum emitters with such a simple yet versatile structure as a gold nanorod are of general fundamental interest and will ultimately lead to design strategies for optimizing molecular fluorescence enhancement.

Photoluminescence from gold nanorods

Benefiting from the presence of the LSPR, apart from strong absorption and scattering, gold nanoparticles also exhibit intense photoluminescence emission. Bulk gold is a very poor light emitter with an emission quantum yield (QY) of $\sim 10^{-10}$, as first discovered by Mooradian [46] in 1969. The weak luminescence originates from the creation of an electron-hole pair in the 5d and 6sp bands of bulk gold. Gold nanoparticles, however, show dramatically increased luminescence emission by the plasmon resonance. It is generally thought that such an increase is a result of a plasmon resonance coinciding with the difference between d-band and sp-band energy levels, increasing the radiative decay rate and therefore increasing the emission quantum yield [47, 48]. The typical quantum yield is in the order of $\sim 10^{-6}$ for gold nanorods [49], several orders of magnitude lower than organic dyes (QY $\sim 10^{-1}$). Photoluminescence emission is further amplified by the large absorption cross-section in the order of $10^{-2}\mu\text{m}^2$, 6 orders of magnitude higher than typical fluorescent molecules.

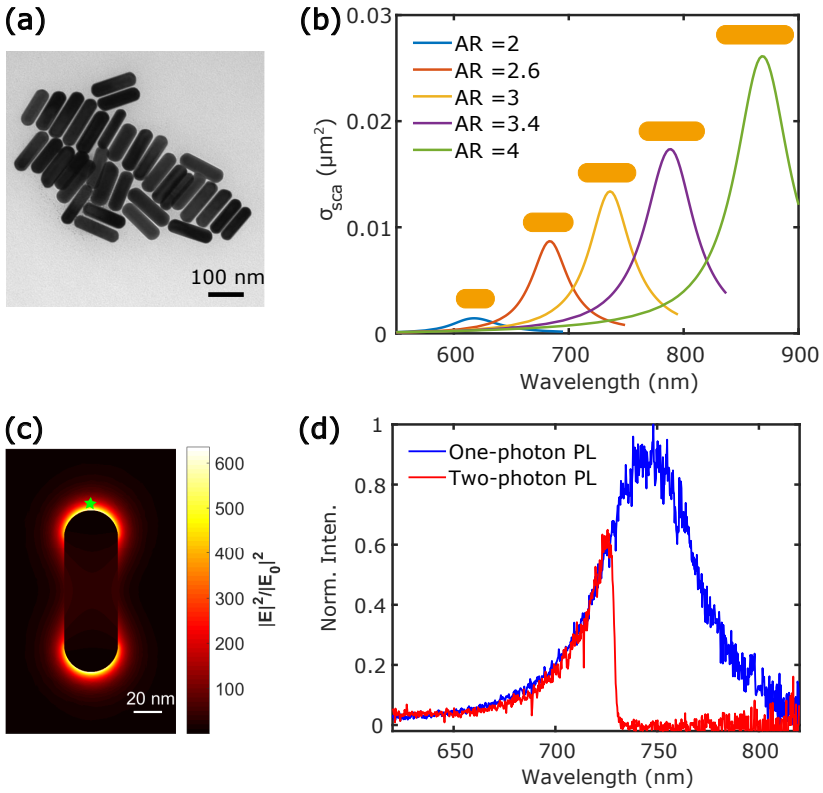

Figure 1.3: **Properties of gold nanorods**. (a) Scanning electron microscopy (SEM) image of gold nanorods. (b) Size dependence of the longitudinal surface plasmon resonance of gold nanorods. The solid lines in different colors plot the calculated (using a discrete dipole approximation method) scattering spectra for gold nanorods of various aspect ratios (ARs) immersed in water. The longitudinal resonance peak shifts to longer wavelengths by increasing the length while keeping a constant diameter of 25 nm. (c) Calculated (using a finite-element method) electric field intensity profile around a 38 nm × 114 nm nanorod in water excited by a circularly polarized plane wave of 775 nm. The green star represents an optical emitter located in the near field of the nanorod. (d) One-photon- and two-photon-excited luminescence spectra measured on a same single gold nanorod immobilized on a glass coverslip and immersed in methanol. Only the blue wing of the two-photon spectrum is present due to a shortpass filter used to cut the excitation laser (775 nm). The spectra have been corrected for the wavelength-dependent response of the optical setup. PL = photoluminescence. See Chapter 4 for the details.

Therefore, the photoluminescence brightness of a gold nanoparticle is comparable with that of a good fluorescent dye molecule.

Due to the plasmonic nature of photoluminescence from gold nanoparticles, the emission spectrum will be particularly enhanced for frequencies around the plasmon resonance. Indeed, previous research has already shown a good resemblance between the luminescence and the scattering spectra of gold nanoparticles [49]. Therefore, throughout this thesis we characterize the plasmon resonance of gold nanorods by measuring the photoluminescence spectra by exciting the interband transition and the transverse plasmon resonance at 532 nm instead of more commonly used scattering spectra. Figure 1.3 (d) shows a typical luminescence spectrum from a single gold nanorod excited by a 532-nm continuous-wave laser.

Photoluminescence of nanoparticles can be excited by both linear and nonlinear absorption. Two-photon- and multi-photon-excited luminescence have been demonstrated by using ultrafast lasers [50–54]. Figure 1.3 (d) shows a typical two-photon luminescence spectrum from a single gold nanorod excited by a 775-nm femtosecond laser. The luminescence from the gold nanorod is usually a background when studying the fluorescence enhancement effect of gold nanorods on fluorescent molecules or quantum dots.

Photothermal reshaping of anisotropc nanoparticles

Since metal nanoparticles have a very low quantum yield, the absorption of light leads to the heating of the nanocrystal, which is known as a photothermal effect. By exciting a nanoparticle at its plasmon resonance, a lot of energy can be absorbed and transformed into heat, and subsequently lead to a high temperature increase for the nanoparticle [55]. Much higher lattice temperature can be reached when the particle is heated by femtosecond laser pulses. The reason is that on longer time scales the nanoparticle starts to exchange its energy with the surroundings and thereby cools itself down [56]. As a consequence, when a femtosecond laser is used to study anisotropic nanoparticles, a major concern is the shape instability of the nanoparticles. At elevated temperatures, anisotropic nanoparticles will transform towards their thermodynamically stable shapes, which are truncated octahedrons determined by the so-called Wulff construction, through surface atom diffusion. Typically, it was found that the reshaping of anisotropic nanoparticles happens at temperatures below the bulk melting point [57–60].

For our applications of gold nanorods for fluorescence enhancement, photothermal reshaping is undesired because when a nanorod deforms towards a more spherical shape its plasmonic properties are lost and the enhancement effect is ruined. Figure 1.4 that the LSPR of a nanorod blue-shifts by 10 nm after irradiated by a femtosecond pulsed laser for 30 s. The LSPR moves farther away from the excitation wavelength, thus the local field is weakened. Severe photothermal reshaping of gold nanorods under ultrafast laser irradiation limits the laser intensity one could use to illuminate molecules and thus limits the number of photons one could collect from single molecules. It makes enhancing two-photon-excited fluorescence much more difficult than enhancing one-photon fluorescence.

1.4. Outline of the thesis

The topic of this thesis is fluorescence enhancement by gold nanorods. In the first part (Chapters 2 to 4), we focus on the enhancement of conventional one-photon-excited fluo-

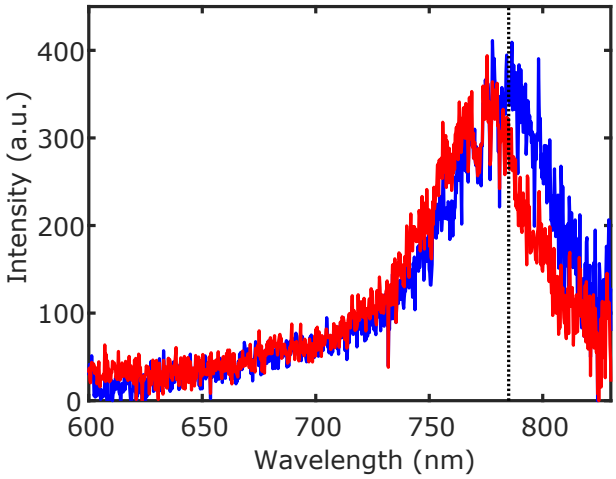

Figure 1.4: **Photothermal reshaping of a gold nanorod**. The blue curve shows the original photoluminescence spectrum ($\lambda_{\mathrm{exc}} = 532$ nm) of a gold nanorod. The nanorod is immobilized on a glass coverslip and immersed in methanol. After irradiated by a femtosecond pulsed laser (785 nm, 6.2 kW/cm^2) for 30 s, the resonance wavelength of the nanorod blue-shifts (red curve) and becomes 10 nm farther away from the excitation wavelength. The dashed vertical line represents the laser wavelength.

rescence and applications. In the second part (Chapters 5 and 6), we work on enhancing nonlinear two-photon-excited fluorescence and luminescence.

Chapter 2. In the studies of interactions between single molecules and metal nanostrctures, reliable and efficient experimental strategies to place the molecule of interest at the right position with respect to the nanostructure with nanometer accuracy are highly desired. In this chapter, we use the free diffusion of single molecules and reversible hybridization of complementary short DNA oligomers (transient binding) as the positioning approach to visualize single-molecule enhancement events. We examine the reliability and photostability of two variants of the transient-binding strategy. We find 3,500-fold fluorescence enhancement of single molecules of IRDye800CW, a near-infrared dye with a low quantum yield of 7%, using single gold nanorods. We also perform numerical simulations for the molecule-nanorod system, which predict consistent enhancement with the experiment.

Chapter 3. This chapter demonstrates an application of fluorescence enhancement. In this chapter, we demonstrate single-molecule electrochemical measurements of the famous redox-sensitive dye Methylene Blue (QY = 4%). Observation of single molecules immobilized on the glass substrate are enabled by the fluorescence enhancement provided by isolated single gold nanorods. The redox state of a single molecule can thus be read out in real time by observing the fluorescence of the molecule as Methylene Blue is fluorescent in the oxidized state and non-fluorescent in the reduced state. Fluorescence blinking induced by redox-state turnovers was studied at different redox potentials on a *same* molecule. The on-off times are found to follow the Nernst equation, through which the mid-point potential of each individual single molecule can be determined.

Chapter 4. In this chapter, gold nanorods are used to enhance anti-Stokes luminescence

of single molecules. The studied anti-Stokes luminescence is a linear optical process where a molecule is excited to the excited state from a vibrational energy level and generates radiation with shorter wavelength than the excitation wavelength. We first characterize the hot-band absorption induced anti-Stokes luminescence of a squaraine dye Seta 670. We then use single gold nanorods to enhance the anti-Stokes luminescence of single Seta 670 molecules and obtain an enhancement factor of 350. Here we rely on the transient sticking of molecules onto the glass substrate to visualize enhancement events.

Chapter 5. In marked contrast to the comprehensive efforts on enhancing the conventional one-photon-excited fluorescence, much fewer attempts have been reported on enhancing two-photon-excited fluorescence/luminescence. Two-photon-excited emission is expected to display much larger signal enhancement since it is proportional to squared intensity of the local electric field. Enhancing two-photon emission is apparently very interesting because of all the advantages and wide-spread applications of two-photon microscopy. However, it turns out much more challenging to enhance two-photon-excited fluorescence of single molecules. The main obstacle is the low emission brightness of common fluorescent dyes, leading to an inadequate number of photons detectable from a single molecule, even if the molecule is close to a gold nanorod. Photothermal reshaping of gold nanorods under ultrafast laser irradiation limits the laser intensity one could use to illuminate molecules. To circumvent this difficulty, in this chapter, we choose to enhance the two-photon-excited luminescence of single quantum dots, which are much brighter with typically three orders of magnitude higher two-photon absorption cross-sections than normal dye molecules. We demonstrate two-photon-excited luminescence enhancement of more than four orders of magnitude for single quantum dots transiently stuck near a single nanorod. We also perform numerical simulations to verify the observed enhancement. The good consistency between simulations and measurements suggests that two-photon luminescence enhancement is not notably affected by the transient broadening of the plasmon resonance after femtosecond excitation. An electromagnetic model is adequate to describe the system.

Chapter 6. In this chapter, we demonstrate two-photon-excited fluorescence enhancement for an ensemble of Rhodamine 6G molecules. By increasing the concentration of fluorescent molecules we are able to detect enough two-photon-excited fluorescence while keeping the laser intensity below the photothermal reshaping threshold of gold nanorods. Our result shows that due to the presence of a single gold nanorod, fluorescence of the molecules in the near field is enhanced, on average, by a factor of 4,500. We find that the enhancement is independent on the excitation power, which further supports that two-photon enhancement is not affected by ultrafast plasmon broadening.

References

[1] J. R. Lakowicz, *Principles of Fluorescence Spectroscopy*, 3rd ed. (Springer US, 2006) p. 954.

[2] W. R. Zipfel, R. M. Williams, and W. W. Webb, *Nonlinear magic: multiphoton microscopy in the biosciences,* Nature Biotechnology **21**, 1369 (2003).

[3] W. Denk, J. H. Strickler, and W. W. Webb, *Two-photon laser scanning fluorescence microscopy,* Science **248**, 73 (1990).

[4] M. Pawlicki, H. Collins, R. Denning, and H. Anderson, *Two-photon absorption and the design of two-photon dyes,* Angewandte Chemie International Edition **48**, 3244 (2009).

[5] A. Diaspro and M. Robello, *Two-photon excitation of fluorescence for three-dimensional optical imaging of biological structures,* Journal of Photochemistry and Photobiology B: Biology **55**, 1 (2000).

[6] M. Rubart, *Two-photon microscopy of cells and tissue,* Circulation Research **95**, 1154 (2004).

[7] M. A. Albota, C. Xu, and W. W. Webb, *Two-photon fluorescence excitation cross sections of biomolecular probes from 690 to 960 nm,* Applied Optics **37**, 7352 (1998).

[8] A. Nag and D. Goswami, *Solvent effect on two-photon absorption and fluorescence of rhodamine dyes,* Journal of Photochemistry and Photobiology A: Chemistry **206**, 188 (2009).

[9] C. Xu and W. W. Webb, *Measurement of two-photon excitation cross sections of molecular fluorophores with data from 690 to 1050 nm,* JOSA B **13**, 481 (1996).

[10] M. Albota, D. Beljonne, J.-L. Brédas, J. E. Ehrlich, J.-Y. Fu, A. A. Heikal, S. E. Hess, T. Kogej, M. D. Levin, and S. R. Marder, *Design of organic molecules with large two-photon absorption cross sections,* Science **281**, 1653 (1998).

[11] K. Podgorski, E. Terpetschnig, O. P. Klochko, O. M. Obukhova, and K. Haas, *Ultra-bright and-stable red and near-infrared squaraine fluorophores for in vivo two-photon imaging,* PloS one **7**, e51980 (2012).

[12] O. V. Przhonska, S. Webster, L. A. Padilha, H. Hu, A. D. Kachkovski, D. J. Hagan, and E. W. Van Stryland, *Two-photon absorption in near-ir conjugated molecules: design strategy and structure–property relations,* in *Advanced Fluorescence Reporters in Chemistry and Biology I* (Springer, 2010) pp. 105–147.

[13] C.-K. Wang, P. Macak, Y. Luo, and H. Ågren, *Effects of π centers and symmetry on two-photon absorption cross sections of organic chromophores,* The Journal of Chemical Physics **114**, 9813 (2001).

[14] C.-L. Sun, Q. Liao, T. Li, J. Li, J.-Q. Jiang, Z.-Z. Xu, X.-D. Wang, R. Shen, D.-C. Bai, Q. Wang, *et al.*, *Rational design of small indolic squaraine dyes with large two-photon absorption cross section,* Chemical Science **6**, 761 (2015).

[15] D. R. Larson, W. R. Zipfel, R. M. Williams, S. W. Clark, M. P. Bruchez, F. W. Wise, and W. W. Webb, *Water-soluble quantum dots for multiphoton fluorescence imaging in vivo,* Science **300**, 1434 (2003).

[16] R. Wood, *Xxix. anti-Stokes radiation of fluorescent liquids,* The London, Edinburgh, and Dublin Philosophical Magazine and Journal of Science **6**, 310 (1928).

[17] M. Orrit and J. Bernard, *Single pentacene molecules detected by fluorescence excitation in a p-terphenyl crystal,* Physical Review Letters **65**, 2716 (1990).

[18] B. Schuler and W. A. Eaton, *Protein folding studied by single-molecule FRET,* Current Opinion In Structural Biology **18**, 16 (2008).

[19] S. Weiss, *Fluorescence spectroscopy of single biomolecules,* Science **283**, 1676 (1999).

[20] X. S. Xie and H. P. Lu, *Single-molecule enzymology,* Journal of Biological Chemistry **274**, 15967 (1999).

[21] W. E. Moerner, *New directions in single-molecule imaging and analysis,* Proceedings of the National Academy of Sciences **104**, 12596 (2007).

[22] R. Roy, S. Hohng, and T. Ha, *A practical guide to single-molecule FRET,* Nature methods **5**, 507 (2008).

[23] E. Rhoades, E. Gussakovsky, and G. Haran, *Watching proteins fold one molecule at a time,* Proceedings of the National Academy of Sciences **100**, 3197 (2003).

[24] C. F. Bohren and D. R. Huffman, *Absorption and scattering of light by small particles* (John Wiley & Sons, 2008).

[25] S. Link and M. A. El-Sayed, *Spectral properties and relaxation dynamics of surface plasmon electronic oscillations in gold and silver nanodots and nanorods,* The Journal of Physical Chemistry B (1999).

[26] P. Zijlstra and M. Orrit, *Single metal nanoparticles: optical detection, spectroscopy and applications,* Reports on Progress in Physics **74**, 106401 (2011).

[27] J. R. Lakowicz, *Plasmonics in biology and plasmon-controlled fluorescence,* Plasmonics **1**, 5 (2006).

[28] J. Pérez-Juste, I. Pastoriza-Santos, L. M. Liz-Marzán, and P. Mulvaney, *Gold nanorods: synthesis, characterization and applications,* Coordination Chemistry Reviews **249**, 1870 (2005).

[29] L. Vigderman, B. P. Khanal, and E. R. Zubarev, *Functional gold nanorods: synthesis, self-assembly, and sensing applications,* Advanced Materials **24**, 4811 (2012).

[30] S. Yao, H.-H. Cai, M. Liu, and P.-H. Yang, *Fluorescent labeling of cellular targets and multicolor imaging with gold nanorods,* Dyes and Pigments **101**, 286 (2014).

[31] P. Zijlstra, P. M. Paulo, and M. Orrit, *Optical detection of single non-absorbing molecules using the surface plasmon resonance of a gold nanorod,* Nature Nanotechnology **7**, 379 (2012).

[32] D. P. O'Neal, L. R. Hirsch, N. J. Halas, J. D. Payne, and J. L. West, *Photo-thermal tumor ablation in mice using near infrared-absorbing nanoparticles,* Cancer Letters **209**, 171 (2004).

[33] X. Huang, I. H. El-Sayed, W. Qian, and M. A. El-Sayed, *Cancer cell imaging and photothermal therapy in the near-infrared region by using gold nanorods,* Journal of the American Chemical Society **128**, 2115 (2006).

[34] X. Huang, P. K. Jain, I. H. El-Sayed, and M. A. El-Sayed, *Plasmonic photothermal therapy (pptt) using gold nanoparticles,* Lasers in Medical Science **23**, 217 (2008).

[35] J. Wenger, *Fluorescence spectroscopy enhancement on photonic nanoantennas,* arXiv preprint arXiv:1709.06749 (2017).

[36] S. Kühn, U. Håkanson, L. Rogobete, and V. Sandoghdar, *Enhancement of single-molecule fluorescence using a gold nanoparticle as an optical nanoantenna,* Physical Review Letters **97**, 017402 (2006).

[37] T. Härtling, P. Reichenbach, and L. Eng, *Near-field coupling of a single fluorescent molecule and a spherical gold nanoparticle,* Optics Express **15**, 12806 (2007).

[38] O. Muskens, V. Giannini, J. Sanchez-Gil, and J. Gomez Rivas, *Strong enhancement of the radiative decay rate of emitters by single plasmonic nanoantennas,* Nano Letters **7**, 2871 (2007).

[39] S. Khatua, P. M. R. Paulo, H. Yuan, A. Gupta, P. Zijlstra, and M. Orrit, *Resonant plasmonic enhancement of single-molecule fluorescence by individual gold nanorods,* ACS Nano **8**, 4440 (2014).

[40] A. Kinkhabwala, Z. Yu, S. Fan, Y. Avlasevich, K. Müllen, and W. Moerner, *Large single-molecule fluorescence enhancements produced by a bowtie nanoantenna,* Nature Photonics **3**, 654 (2009).

[41] D. Punj, M. Mivelle, S. B. Moparthi, T. S. van Zanten, H. Rigneault, N. F. van Hulst, M. F. Garcia-Parajo, and J. Wenger, *A plasmonic 'antenna-in-box' platform for enhanced single-molecule analysis at micromolar concentrations,* Nature Nanotechnology **8**, 512 (2013).

[42] G. Acuna, F. Möller, P. Holzmeister, S. Beater, B. Lalkens, and P. Tinnefeld, *Fluorescence enhancement at docking sites of DNA-directed self-assembled nanoantennas,* Science **338**, 506 (2012).

[43] P. Anger, P. Bharadwaj, and L. Novotny, *Enhancement and quenching of single-molecule fluorescence.* Physical Review Letters **96**, 113002 (2006).

[44] H. Yuan, S. Khatua, P. Zijlstra, M. Yorulmaz, and M. Orrit, *Thousand-fold enhancement of single-molecule fluorescence near a single gold nanorod.* Angewandte Chemie International Edition **52**, 1217 (2013).

[45] X. Nan, P. A. Sims, and X. S. Xie, *Organelle tracking in a living cell with microsecond time resolution and nanometer spatial precision,* ChemPhysChem **9**, 707 (2008).

[46] A. Mooradian, *Photoluminescence of metals,* Physical Review Letters **22**, 185 (1969).

[47] E. Dulkeith, T. Niedereichholz, T. Klar, J. Feldmann, G. Von Plessen, D. Gittins, K. Mayya, and F. Caruso, *Plasmon emission in photoexcited gold nanoparticles,* Physical Review B **70**, 205424 (2004).

[48] C. Sönnichsen, T. Franzl, T. Wilk, G. von Plessen, J. Feldmann, O. Wilson, and P. Mulvaney, *Drastic reduction of plasmon damping in gold nanorods,* Physical Review Letters **88**, 077402 (2002).

[49] M. Yorulmaz, S. Khatua, P. Zijlstra, A. Gaiduk, and M. Orrit, *Luminescence quantum yield of single gold nanorods,* Nano Letters **12**, 4385 (2012).

[50] C. Molinaro, Y. El Harfouch, E. Palleau, F. Eloi, S. Marguet, L. Douillard, F. Charra, and C. Fiorini-Debuisschert, *Two-photon luminescence of single colloidal gold nanorods: revealing the origin of plasmon relaxation in small nanocrystals,* The Journal of Physical Chemistry C **120**, 23136 (2016).

[51] H. Wang, T. B. Huff, D. A. Zweifel, W. He, P. S. Low, A. Wei, and J.-X. Cheng, *In vitro and in vivo two-photon luminescence imaging of single gold nanorods,* Proceedings of the National Academy of Sciences of the United States of America **102**, 15752 (2005).

[52] M. Eichelbaum, B. Schmidt, H. Ibrahim, and K. Rademann, *Three-photon-induced luminescence of gold nanoparticles embedded in and located on the surface of glassy nanolayers,* Nanotechnology **18**, 355702 (2007).

[53] R. A. Farrer, F. L. Butterfield, V. W. Chen, and J. T. Fourkas, *Highly efficient multiphoton-absorption-induced luminescence from gold nanoparticles,* Nano Letters **5**, 1139 (2005).

[54] P. Zijlstra, J. W. Chon, and M. Gu, *Five-dimensional optical recording mediated by surface plasmons in gold nanorods,* Nature **459**, 410 (2009).

[55] A. O. Govorov and H. H. Richardson, *Generating heat with metal nanoparticles,* Nano today **2**, 30 (2007).

[56] G. Baffou and H. Rigneault, *Femtosecond-pulsed optical heating of gold nanoparticles,* Physical Review B **84**, 035415 (2011).

[57] A. B. Taylor, A. M. Siddiquee, and J. W. M. Chon, *Below melting point photothermal reshaping of single gold nanorods driven by surface diffusion,* ACS Nano **8**, 12071 (2014).

[58] P. Zijlstra, J. W. Chon, and M. Gu, *White light scattering spectroscopy and electron microscopy of laser induced melting in single gold nanorods,* Physical Chemistry Chemical Physics **11**, 5915 (2009).

[59] W. Albrecht, T.-S. Deng, B. Goris, M. A. van Huis, S. Bals, and A. van Blaaderen, *Single particle deformation and analysis of silica-coated gold nanorods before and after femtosecond laser pulse excitation,* Nano Letters **16**, 1818 (2016).

[60] P. Buffat and J. P. Borel, *Size effect on the melting temperature of gold particles,* Physical Review A **13**, 2287 (1976).